2 Literature Review

2.1 Introduction

The BBC World Service owns and hires MF and HF transmission sites for its international broadcasting services, where short wave propagation is via earth F^2-layer ionosphere refractions. The transmitters are typically of high power (between 250 and 500kW), broadcasting through high gain curtain antennas. At such sites, the BBC is obliged to consider the potential risk to its staff and members of the public posed by radiation from the high power transmitting antennas. The near field region, close to these antennas is of particular interest from the point of view of both occupational and public exposure to high RF fields. This is because station boundary fences can be within one or two wavelengths of the antenna, so the ability to analyses or model the near field region is important for demonstrating compliance with accepted guidelines. Guidelines for occupational and public exposure are different. The occupational guidelines assumed that the individual is of working age and in good health. It is reasonable to assumed that people who are exposed to radiation through their occupation will be familiar with the equipment and have received adequate training [2.1]. The public exposure guidelines assume that the hazard is presented to a person of any age and in any state of health. It is also unlikely that the public will be aware of the hazards or the existence of high levels of radiation.

The main objectives of this research are to understand and find a computationally efficient method for the analysis and prediction of these exposure levels in compliance with International Commission on Non-Ionising Radiation Protection (ICNIRP) human exposure guidelines [2.2]. This is necessary to understand the correlation between energy absorption rates in the body and the risk to health, as well as near-field distributions of the high power BBC HF broadcasting transmission site.

This chapter provides some background information about the broadcasting antenna arrays and summarizes basic principles of human exposure safety guidelines. Further safety criteria required by ICNIRP will be described in following chapter.

A range of research studies are presented. The common objective is to build a modelling and measurement methodology to assess compliance with ICNIRP EM exposure guidelines in close proximity to HF transmitting antennas. This chapter gives a brief review of background information about broadcasting sites and International guidelines on human RF exposure.

Near field RF conditions are assessed through the use of efficient and accurate numerical methods, some of which are present in this chapter. They can provide an insight into how the near field characteristics can be disturbed by the presence of a person. Two software packages were used to model curtain antennas, Numerical Computational Code 4 (NEC4) [2.3] and CST Microwave Studio [2.4]. The theory behind these packages are briefly summarised in Section 2.2. Several software packages are available on the market and it is beneficial for the user to have some knowledge of the software engines which they employ and to understand the basic equations and application methods used by the different numerical codes.

Human phantoms – high resolution numerical models of human beings which incorporate the electrical properties of the body and its internal organs - are described in this chapter. The software package SEMCAD and its associated 'Virtual Family' of human phantoms are introduced. Results generated with the Virtual Family [2.5] associated with the SEMCAD package [2.6] are compared with earlier results generated using a phantom called 'Norman'- Normalised Man, a model developed by the UK HPA (Health Protection Agency – Radiation Protection Division). The different capabilities and limitations of all these numerical codes are described, and finally a description of an equivalence principle theory is given. The equivalence principle was used as part of a hybrid approach to develop a modelling methodology to solve this EM problem.

This chapter is divided into two sections. First HF broadcasting antenna and background ICNIRP guidelines, then numerical methods and techniques / Simulation Software

2.1.1 BBC HF antennas

Until recently, short-wave broadcast transmitters operate in the frequency range 3MHz to 30MHz. The BBC World Service owned and operated 7 high power transmitting

stations, worldwide, through a contract with Babcock International Group. The BBC world service uses frequencies between 5 MHz and 23 MHz. The pertinent details are given in Table 2.1.

Site		Senders	Power(kW)	Antennas	Location
Ascension Island		6	250	7 fixed	14º23'W 07º54'S
				22 slewable	
Oman	(A'Seelah A)	2 (MF)	800	2 slewable	59º34'E 21º51'N
	(A'Seelah B)	3	250	6 curtain	21º51'N 59º34'E
				1 rotatable	
Cyprus	(Lady's Mile)	2 (MF)	500	2 fixed	33º00'E 34º40'N
	(Zygi)	1 (MF)	200	1 fixed	33º19'E 34º43'N
		4	300	22 slewable	
		6	250	5 fixed	
Seychelles		4	250	6 slewable	55 28'E 04 36'S
Singapore	(Kranji)	4	100	1 fixed	103º44'E 01º24'N
		5	250	20 slewable	
Thailand(Nakon Sawan)		5	250	4 fixed	100º04'E 15º03'N
				11 slewable	

Table 2.1 BBC world Service transmitting MF/HF sites [2.7]

The MF antennas are usually array and uses tower as vertical radiators. HF broadcasting antennas are mainly horizontally polarized curtain or broadside arrays. Occasionally log-periodic antennas are used. Babcock International Group also operates HF stations on behalf of the BBC World Service in the UK. These stations are located at Rampisham (Dorset), Woofferton (Shropshire), and Skelton (Cumbria). Currently the transmission frequencies at these sites are in the 4 MHz, 6 MHz, 7 MHz, 9 MHz, 11 MHz, 13 MHz, 15 MHz, 17 MHz and 21 MHz broadcast bands [2.7], more details can be found in Appendix A-1.

Fig 2.1 A'Seelah (Oman) Transmitting station rotatable HF curtain array

The antennas are nearly all horizontally polarized curtain arrays, supplied by a limited number of manufacturers. The differences between these curtain arrays are however quite small. In each case a self-supporting tower is generally used. Some stayed masts are also in use. In Oman a rotatable HF curtain array has been installed which can be seen in Fig 2.1.

A curtain array consists of a vertical matrix of co-planar horizontal dipole elements. Usually a reflecting screen is placed behind each of the dipoles. In this type of antenna the main beam is directed orthogonal to the matrix. The antenna will often be capable of operating over a bandwidth of up to about 2:1. The arrays typically consist of 16 half-wave dipoles, 4 wide and 4 high. But 2 x 4 and 4 x 2 arrays are also in use. The dipoles are usually folded and driven from vertical open-wire balanced feeders [2.8]. Connected in this way dipoles are nominally operated in phase with one another. But by offsetting the phase of the vertical feeders the beam, can be slewed horizontally. Due to logistical considerations the modelling and measurement studies were conducted at the Skelton (Penrith, Cumbria, UK) transmitting station as depicted in Fig 2.2 Birdview of Skelton (Cumbria, UK) transmitting station C site

The Skelton transmitting station was originally built by the BBC in 1942 to provide short wave service to Europe. It covers an area of 750 acres at a height of 600 feet above sea level. It was once the largest and most powerful radio station in Europe [2.9]. The Skelton site is now owned and operated by the Babcock International Group, who took over from Merlin Communications International Ltd who themselves acquired the station following the privatisation of BBC Transmission in 1997.

Fig 2.2 Birdview of Skelton (Cumbria, UK) transmitting station C site.

Babcock International Group staff at the Skelton Transmitting Station used in thesis have been very helpful and supportive of this research. The antenna model used in this project was based on original drawings of the Skelton antenna supplied by Marconi Communications. The curtain array used in this study is the Skelton C wide slew HF antenna array 766 (Type R9010, HRS 4/3/0.5λ[1]).

In short wave broadcasting services, there are two field regions which extend to near ground level:

- The reactive near-field region of an antenna, $r \leq \frac{\lambda}{4}$;
- The Fresnel field region of an antenna,$r > \frac{\lambda}{4}$;

[1]Curtain antennas are categorised as :HRRS n/m/h
H- Horizontal; R- Array with Reflector; R- Also Reversible (if second "R" present); S- Slewable; n- number of rows of dipoles; m- number of columns of dipoles;
h- height above ground of lowest row of dipoles (in wavelength)

Where *r* is the distance from the centre of the antenna to the point of investigation.

Fig 2.3 Vatican Radio antenna towers [2.10].

As can be seen in Fig 2.2 most of these high powers broadcasting transmitter stations are located in unpopulated rural areas. Metal fences and locked gates help to keep the public a certain distance away from these arrays. There are also some unusual and uncontrollable cases in short-wave broadcasting. Fig 2.3 Vatican Radio antenna towers Fig 2.3 Vatican Radio antenna towers [2.10] shows the periphery of the transmitter station for the Vatican Radio station, which is near Cesano, 12 miles north of Rome. It is clear from the figure that this station is surrounded by a populous residential area. Similarly in Singapore the Kranji transmitter station is located on land adjacent to the main building of a Golf club. To maximize the coverage area MF band (300 kHz-3MHz) and HF band (3 MHz - 30 MHz) broadcasting transmitters all operate at high power (Table 2.1), details which can be found in Appendix A-2.

Numerous international scientists have researched the possible health hazards associated with human exposure to EMF. Recently many of these studies have focused primarily on the modern telecommunications systems, such as cellular Base Stations. Studies in this area include those conducted in 2006 by Mobile Telecommunications and Health Research (MTHR) [2.11], and the German Mobile Telecommunication Research Programme conducted by The German Commission on Radiological Protection [2.12]. After a review of these recent studies the ICNIRP concluded that

exposure levels due to cell phone base stations are generally around one-ten-thousandth of the guideline levels [2.13]. A statement on the topic was published in 2009 by the ICNIRP. It was entitled "Guidelines for limiting exposure to time-varying electric, magnetic, and electromagnetic fields (up to 300 GHz)" [2.14]. It indicated that there is a lack of satisfactory individual exposure assessment of low-level, whole-body exposure in the far-field of radiofrequency (RF) transmitters. A problem for those such as the BBC World Service and Vatican Radio, are the possible high levels of whole-body exposure in the near-field of HF high power broadcasting transmitting stations; there have not been many studies done on this so far. In 2006, the European Broadcasting Union published the results of a study carried out by the United Kingdom Health Protection Agency (UK HPA) and commissioned by the BBC World Service. The purpose of the study was to assess the emission compliance of the BBC MF [2.15] and HF [2.16] broadcast transmitters against the ICNIRP exposure guidelines. The HPA applied Finite Difference Time Domain (FDTD) solution of Maxwell's curl equations to compute the whole body Specific Absorption Rate (SAR). In addition, a quasi-static Scalar Potential Finite Difference (SPFD) solution of Laplace's equation was used to compute limb SAR as a function of the induced current [2.17], [2.18]. This was then linked to the whole body incident field strength through the FDTD algorithm. A human phantom was illuminated with either a vertically or horizontally polarized plane wave, in various configurations such as: bare-feet touching the ground, with shoes, isolated; arms at the side, or outstretched [2.15], [2.16]. It was assumed that in the near-field of an MF antenna the dominant field component is a uniform and vertically polarized electric field. In this case, the localised SAR in the leg is the most restrictive quantity [2.2], [2.15].

Prior to these studies by the HPA there was a very limited amount of research which involved comparing the emission from broadcasting antennas against the ICNIRP guidelines. Other HPA studies formed the foundation for the guidelines published by the ICNIRP in 1998. In 1994 Jokela *et al* measured the emissions from a MF vertical monopole antenna operating at a frequency of 963 kHz with an input power of 600 kW [2.19]. This antenna is located in Pori (Finland). Through measurement Jokela *et al* discovered that the electric field was 500V/m at 1m above the ground. At 10 m the E-field strength was found to be 90 V/m. These measurements were made at a distance of 40 m in front of the antenna [2.20]. Jokela *et al* calculated the current flowing through

the feet of a grounded hemispheroidal model of human. The vertical electric field induced a current of 140mA at 10m away from the antenna and 30mA at 40 m away from the antenna. Jokela *et al* also measured the RF exposure in front of a 500kW HF curtain array which was operating at 21.55 MHz. The antenna in question is also located at the Pori broadcasting station. They measured maximum values of electric field strength and induced current through feet of a grounded human model of 90 V/m, 400mA at a distance of 30 m in front of the antenna. At a distance of 100 m in front of the antenna they measured 35 V/m, and 75mA. In each case the measurements were obtained at a height of 1 m above the ground. From 1989 to 1998 Mantiply *et al* conducted a series of similar electric field strength measurements [2.21]. Mantiply studied the exposure level in a community located 10km from six 250 kW HF transmitters. These transmitters were used to service the Voice of America's (VOAs) Delano site in California, United States. These transmitters operate at four different frequencies, namely: 6.155 MHz, 9.765 MHz, 9.815 MHz, and 11.74 MHz [2.22]. Moreover the electric field strength was measured in front of three other 100kW HF antennas at distances of 100m, 200m and 300m. These distances were measured 1m above the ground in the direction of wave propagation. An electrically steerable curtain antenna (slewable angle $\pm 25^{\circ}$) was also investigated [2.22]. These studies assessed the EMF level in front of the high power MF and HF antennas. Specifically the E-field was examined at distances ranging from 10m-10km. The study provides data on the range of fields values associated with several different types of HF sources. However it did not provide sufficient information to assess the potential human exposure to the intense level of HF field.

2.1.2 International Exposure Guidelines and Basic Definitions

Human exposure to electromagnetic radiation is of concern to individuals and organisations worldwide in relation to the functioning of telecommunications systems. There are established standards to prevent overexposure to the electromagnetic fields, present in our environment. Exposure standards for radiofrequency energy have been developed by various organizations and countries. These standards recommend safe levels of exposure for both the general public and for workers. The International Commission on Non-Ionizing Radiation Protection (ICNIRP) is a non-governmental organization, formally recognized by World Health Organisation (WHO). The

independent scientific experts of the ICNIRP review and evaluate scientific research literature from all over the world [2.14].

Other countries and regions have taken similar precautions. For example, Canada has adopted a set of SAR guidelines entitled 'Limits of Human Exposure to Radiofrequency Electromagnetic Energy in the Frequency Range from 3 kHz to 300 GHz - Safety Code 6' [2.23]. This document sets out the requirements and measurement techniques to be followed when evaluating RF exposure. On the other hand in the United States, on the other hand, the Federal Communication Commission (FCC) has adopted safety guidelines for evaluating RF environmental exposure. These guidelines which have been in place since 1985 [2.24], [2.25]. They were derived from guidelines produced by the National Council on Radiation Protection and Measurements (NCRP) and the Institute of Electrical and Electronics Engineers (IEEE). Many countries in Europe and elsewhere in the world use exposure guidelines developed by the ICNIRP [2.2], [2.14]. The ICNIRP safety limits are generally similar to those of the NCRP and IEEE [2.26], [2.27], with a few exceptions. For example, the ICNIRP recommends different exposure levels in the lower and upper frequency ranges and for localized exposure due to devices such as hand-held cellular telephones. The NCRP, IEEE and ICNIRP exposure guidelines identify the same threshold level at which harmful biological effects may occur. These levels are the basic restrictions.

2.1.3 SAR and Current Density

The Specific Absorption Rate, or SAR, is the rate at which RF energy is absorbed by a defined amount of mass of a biological body. It is a time derivative of the incremental energy (dW) absorbed by (i.e. dissipated in) an incremental mass (dm). This incremental mass is contained within a volume element (dV) of a given density (ρ) shown in equation (2.1) [2.28]. The density is measured in units of watts per kilogram (W/kg). It is a value averaged over pre-defined mass, seen as [2.28]:

$$SAR = \frac{d}{dt}\left(\frac{dW}{dm}\right) = \frac{d}{dt}\left(\frac{dW}{\rho dV}\right) \tag{2.1}$$

It can also be written as (Equation 2.2):

$$SAR = \frac{P}{\rho} = \frac{\sigma E^2}{2\rho} = \frac{J^2}{2\rho\sigma} \tag{2.2}$$

where: P = Power loss density

E = Electric field strength

J = Current density

σ = Conductivity

ρ = tissue density

To obtain the whole-body averaged SAR the absorption rate in all the cells of the computational volume must be summed together and then divided by the mass of the whole body. The averaged SAR, $\bar{S}$, is given by equation (2.3) [2.29]:

$$\bar{S} = \sum_{i=1}^{N} S_i \rho_i \left(\sum_{i=1}^{N} \rho_i \right)^{-1} \tag{2.3}$$

when working with a multilayer cylinder phantom the SAR can be averaged over the volume of each layer. The equation (2.4) can be written as follows [2.30]:

$$\bar{S} = \sum_{i=1}^{N} S_i V_i \left(\sum_{i=1}^{N} V_i \right)^{-1} \tag{2.4}$$

Where N is the number of the layers in the cylinder phantom S_i is the SAR value computed in the volume of each cylinder i.

The whole-body averaged SAR is the mean of a distribution which depends on the frequency, polarization, and the zone of the incident field region. The calculations also depend on the mass and geometry of the biological body. When the power density of an incident electromagnetic yield is increased, then the relative increase of the whole-body SAR will be directly proportional to the increase of any part-body SAR [2.28].

The currents and energy absorption in human body tissue depend on the coupling mechanisms and the frequency involved. The electric field and current density within the tissue can be determined by Ohm's Law: $J = \sigma E$, where J is the current density in A/m^2, σ is the electrical conductivity of the medium in S/m, and E is the electric field strength in V/m. The dosimetric quantities used in by the IEEE and ICNIRP, for different frequency ranges and waveforms are as follows (Table 2.2):

Quantities	unit	Frequency range
Current density	J(A/m^2)	up to10 MHz
Current	I(A)	up to 110 MHz
SAR	SAR (W/kg)	100 kHz-10 GHz
Power Density	S (W/m^2)	10-300GHz

Table 2.2 Summary of EMF and dosimetric quantities and units used in these ICNIRP guidelines[2.20]

2.1.4 Basic Restrictions and Reference Level

The ICNIRP provides global safety standards for radio frequency emissions. This identifies the main adverse effect of exposure to EM fields between 100 kHz and 10GHz as being from body tissue temperature rise. Thermal effects (tissue heating) can cause biological damage to the human body especially in some parts of the body which are more sensitive to the changes [2.31], [2.32]. Significant damage can occur in eyes, testis and neural functions. Frail and/or elderly people, young children and people with medical conditions are often less resistant to exposure by intense EM fields [2.33], [2.34]. These thermal effects are caused by electromagnetic energy being absorbed by human tissue [2.32].

The ICNIRP guidelines set limits for human exposure based on SAR and current density in the body. The human body absorbs energy from electromagnetic fields (EMFs) at frequencies between 100 kHz to 300 GHz. This leads to induced internal electric fields and currents within the body, which have adverse biological effects. These adverse effects are: excessive heating, electric shock and burns. The electric and magnetic field strengths are the reference level for the external exposure in time-varying EMF. At frequencies above 10 GHz the surface of the human body absorbs energy from thE-field which could lead to excessive surface heating. It also is defined as the reference level for that EMF spectral region. Dr Paolo Vecchia, a member and chairman of the ICNIRP committee has explained [2.35] that any effects that might result in health hazards can account for the choice of definition for the basic restrictions. He also explained that the basic restriction were recommended by the ICNIRP as well as other international standards; they were considered the appropriate biologically effective quantities and set below the threshold for the appropriate critical effects [2.35]. The limits were established either through experimental or computational dosimetric techniques. Recommended reference levels are derived from

the basic restrictions. Different limits are set for ‘occupational’ and ‘public’ exposure arguing that anybody exposed under occupational conditions will be of a certain age and fitness level while the public might include anybody. As well as the Basic Restrictions which are based on energy absorption, ICNIRP defines Reference levels of EM Field Strength. ICNIRP points out that, in general, if the EM Field Strength is below the Reference Level it can be assumed that the basic restriction will not be breached [2.2], [2.20].

	Basic restrictions					Reference levels		Reference levels at 6MHz
	*f	Current density ($mA/m^{2)}$ (rms)	**WBSAR (W/kg)	Localized SAR for head and trunk (W/kg)	Localized SAR for limbs（W/kg)	*f	E-field (V/m)	E-field (V/m)
Occupational exposure	100kHz-10MHz	f/100	0.4	10	20	1-10MHz	610/f	101
	10MH-10GHz	—	0.4	10	20	10-400MHz	61	61
General public exposure	100kHz-10MHz	f/500	0.08	2	4	1-10MHz	87/f1/2	35
	10MH-10GHz	—	0.08	2	4	10-400MHz	28	28

Table 2.3 ICNIRP basic restrictions and reference levels for HF frequency band [2.2]

*f as indicated in the frequency range
**WBSAR: Whole-body average SAR

The ICNRP requires that the localized SAR is averaged over any 10g of contiguous tissues. ANSI/IEEE whole-body SAR is averaged over the entire body, and partial-body SAR is averaged over any 1g of tissue defined as a tissue volume in the shape of a cube. SAR for hands, wrists, feet and ankles is averaged over any 10g of tissue defined as a tissue volume in the shape of a cube. Different exposure limits are applied to some devices when only part of the human body is exposed to the radiation. Such limits apply to mobile phones and base stations. Numerous research studies have been carried out to assess human exposure to these low power devices. T.G. Cooper *et al* [2.36] of the United Kingdom National Radiation Protection Board (NRPB) measured the radio wave power density in the vicinity of 20 U.K. Microcell and Picocell mobile base stations. He summarized his finding in a report on general public exposure. In 1994 P.J. Dimbylow and S. Mann constructed a human head model from MRI scan slices [2.37]. They then applied the Finite Differential Time Domain (FDTD) technique to calculate SAR in the head model expose in an early mobile handset model. In 2009 Martínez-Búrdalo, M *et al* [2.38] also used FDTD to assess the human exposure to EMF from wifi and Bluetooth devices. They used a XFDTD platform generated by REMCOM [2.39] and another magnetic resonance imaging (MRI) image based upon a human head model produced by the Hershey Medical Centre in Pennsylvania, United States. The next section of this thesis provides further details on the limits specified in the exposure guidelines.

2.1.5 Voxel Phantoms

A phantom is used to model the human body and evaluate the risks associated with human exposure to RF fields. The phantom could be either a physical or numerical model of the whole body or of specific organs. Various types, methods, materials types of phantom have been developed to model the electrical properties of a human.

Through theoretical studies and analysis, earlier researchers have developed simple human models. In 1979 Habib Massoudi developed multi-layered cylindrical models of men. These models were used to study the absorption of energy from plane waves at frequencies between 0.4 GHz and 8 GHz [2.30]. In 1980 I Chatterjee used multi-layered slab models in conjunction with the plane wave spectrum (PWS) technique to calculate the energy absorption at 2.45 GHz [2.40]. Around the same time, another relatively coarse inhomogeneous human model was used to calculate SAR [2.41],

[2.42]. This model consisted of various blocks having dielectric properties that matched those of several human organs. The technique involved the use of the Method of Moments (MoM) Since the 1990s advanced medical diagnostic techniques, such as magnetic resonance imaging (MRI), computed tomography (CT) etc. have been employed to develop realistic high resolution voxel models. Human coupling with the induced field are the main cause for the human biology reactions. The factors of effects have been quantified as SAR, induced electric field, and current density. These quantities depend on the frequency of the applied RF field and tissue type (i.e. dielectric properties). In order to study and understand the correlation between these physical quantities and the induced biological response, the simulations calculate a region of specific tissue mass for averaging. In order to obtain more accurate results a human phantom incorporating greater spatial detail is required. Moreover, the age, gender and posture of exposed limbs were studied in order to gain a better understanding of their relevance in the risk assessment [2.43], [2.44], [2.45]. The exposure problem associated with modern communication systems has become more complicated as technologies have developed in the past 10 years. High resolution anatomical human phantoms play an important role in evaluating the risk associated with human exposure to RF fields. These models are used in the calculation of SAR, induced electric field and current density. Chapter 3 provides a more detailed description of the human phantoms have been used in this research.

2.2 Numerical Methods and Techniques

The NEC4 modelling package is based on the Method of Moments, which is an efficient and accurate technique; it is more suited to model wires and linear dielectrics. SEMCAD and CST microwave studio are commercial simulation packages based on finite element codes. These codes are suited to modelling complex inhomogeneous geometries such as the human body. However, compared with NEC4, these packages are very expensive and inefficient for modelling large electrical radiation problems. In fact none of the commercial codes currently available are well suited to this electromagnetic problem studied in this thesis. The array and its surrounding structure and environments are electrical large and complex. SEMCAD has advantage of SAR calculation but less efficient on the field distributions investigation. CST did not have human phantom until earlier 2011. It is impractical to measure the SAR, induced

electric field, or current density within a human body directly. For this reason the evaluation of SAR within a human body is generally based on results obtained through numerical modelling and simulation. It is helpful to correlate the results obtained through different approaches in order to validate the simulated and derived results. The following subsections aim to give a basic introduction to the numerical techniques which form the foundation of several commercial simulation packages, such as CST Microwave Studio, [2.4], SEMCAD [2.6], and NEC4 [2.46].

2.2.1 Method of Moments

The method of moments was developed by Roger F. Harrington [2.47]. The Laurence Livermore National Labs devised efficient ways to use the method of moments to solve problems that arise during the design of wire and wire array antennas. NEC4 is a numerical code written in FORTRAN with a single interface [2.46], and has been widely used to model wire based antennas. New developments have extended the applications of MoM to enable 3D EM modelling of wires and flat PEC scatters, through the use of a triangular mesh [2.48]. The MoM applies orthogonal expansions to translate the integral equations into a set of simultaneous linear equations. Basis functions and coefficients matrix methods are used to expand, invoke and solve the current distributions [2.49]. The procedure to find a solution begins by defining the unknown current distribution $I_z(z')$ in terms of an orthogonal set of basic functions. Sub-domain basis functions are used to subdivide a wire into small segments and model the current distribution on each [2.47]. The shape of the sub-domain basis functions can vary depending on geometry of the objects to be modelled. Typically rectangle, triangle, or sinusoidal basis functions are used in MoM. The amplitude of these constructs is represented using expansion function coefficients, while a Fourier series is used to represent the current distributions along the entire wire[2.3]. Finally the antenna's radiation characteristics and feed point impedance are derived from the calculated current distribution (equation 2.5 and 2.6).

$$\sum_{n=1}^{N} C_n G_n(z) = E_z(z) \tag{2.5}$$

where

$$G_n(z) = \frac{1}{j4\pi\omega\epsilon}\int_{-\frac{l}{2}}^{l/2} F_n(z')\left[\frac{\partial^2}{\partial z^2} + k^2\right]\frac{e^{-jkR}}{R}dz' \qquad (2.6)$$

C_n = expansion coefficient associated with the current

$F_n(z')$ = basis function

The boundaries conditions are satisfied by solving the integral equation obtained through the use of Green's functions. The electric field integral equation 2.7 (EFIE) and Magnetic field integral (equation 2.8) (MFIE) are the primary formulations of MoM which can be derived from Maxwell Equations [2.3].

EFIE $$E = fe(J) \qquad (2.7)$$

MFIE $$H = fm(J) \qquad (2.8)$$

Where E = the electric field Strength integral equation, H = the magnetic field strength integral equation and J equals the induced current.

After introducing the integral equation into equations (2.5) and (2.6) we obtain two new equations 2.9 and 2.10:

$$\sum_{n=1}^{N} C_n < H_m(z)G_n(z) >=< H_m(z)E_z(z) > \qquad (2.9)$$

$$< H_m(z)G_n(z) >= \int_{-\frac{l}{2}}^{l/2} H_m(z)G_n(z)dz \qquad (2.10)$$

Where $H_m(z)$ is the testing function has a non-zero value for only a small segment of wire located at $z=z_m$. This operation yields a set of integral equations (Equation 2.11-2.14) and can be written in matrix form as

$$[Z_{mn}][I_n] = [V_m] \qquad (2.11)$$

Where

$$Z_{mn} = \int_{-\frac{l}{2}}^{l/2} H_m(z)G_n(z)dz \qquad (2.12)$$

$$I_n = C_n \qquad (2.13)$$

$$V_m = \int_{-\frac{l}{2}}^{l/2} H_m(z) E_z(z) dz \tag{2.14}$$

The linear equations will yield the value of C_n

$$[I_n] = [Z_{mn}]^{-1}[V_m] \tag{2.15}$$

The unknown induced current $I_z(z')$ is now obtained by solving the system of equation (2.15), given above [2.3]. Other parameters such as the scattered electric and magnetic fields can be calculated directly from the induced currents. However the Numerical Electromagnetics code (NEC), is a MoM based code that is mainly used to solve problems involving sets of linear elements or PEC plate scatters such as wires and patches. It is very efficient when applied to volume dielectric objects such as homogeneous multi-layer biological human models. Unfortunately it cannot handle inhomogeneous phantoms. However the NEC method supports the rapid analysis of wire conductors. This makes it suitable for modelling HF curtain arrays efficiently. Since SAR is the main concern in human exposure research, chapter 3 will show how this SAR can be analysed using the FDTD and FEM methods.

2.2.2 Finite Difference Time Domain Method

In 1966Yee implemented interleaved components in a Cartesian grid. In 1975 Taflove introduced a stability criteria along with a 3D grid [2.50]. In 1980 Taflove coined the term Finite Difference Time Domain (FDTD) method [2.51]. In 1981 Mur developed absorbing boundary conditions [2.52]. By the 1990's sufficient computer processing power was available to handle complex problems. The FDTD method is intuitive to use, easy to implement, robust and flexible. Consequently it is used in a wide variety of applications and can also handle complex and heterogeneous objects. Effectively the FDTD method represents a direct solution of Maxwell's time dependent curl equations (2.15 and 2.16), which can be written as follows[2.53]:

$$\frac{\partial \vec{B}}{\partial t} = -\nabla \times \vec{E} - \vec{J}_m \tag{2.16}$$

$$\frac{\partial \vec{D}}{\partial t} = -\nabla \times \overrightarrow{EH} - \vec{J}_e \tag{2.17}$$

where *H* is the magnetic field intensity (A/m),

E is the electric field intensity (V/m),

B is the magnetic flux density (W/m ²),

D is the electric flux density (D/m ²),

$\vec{J}_m$ is the magnetic current (V/m ²),

$\vec{J}_e$ is the electric current (A/m ²).

The FDTD algorithm is based on a description of the time stepping procedure as described in equations 2.15 and 2.16. Fig. 2.4 depicts the position of two interleaved grids of discrete points. One point contains evaluated electric field (yellow) components in the primary Yee cell while magnetic field (green) components are evaluated in a secondary Yee cell. Both are allocated within the staggered Cartesian grid. Each of the E-field vector nodes is surrounded by field components on the basis of a finite central difference approximation and corresponding to the Faraday and Ampere's Law. The i, j, k axis of the FDTD grid represent a 3D volume element. These axes are aligned with the x, y, z axes of the Cartesian grid.

The discretization in time, required to implement the FDTD method, is performed in a leap-frog manner by application of a temporally shifted update of the E and H field components [2.53]. This is illustrated in Fig. 2.5.

Thereby the E-field components are calculated at a time increment t = (n+l)Δt, (l = 0, 1, 2 ...) [2.53]. The computation of the H field components in FDTD method is performed at t = (n + l + 1/2) Δt , (l = 0, 1, 2 ...), i.e. shifted by half a time step. The time step Δt is defined by equation 2.16.

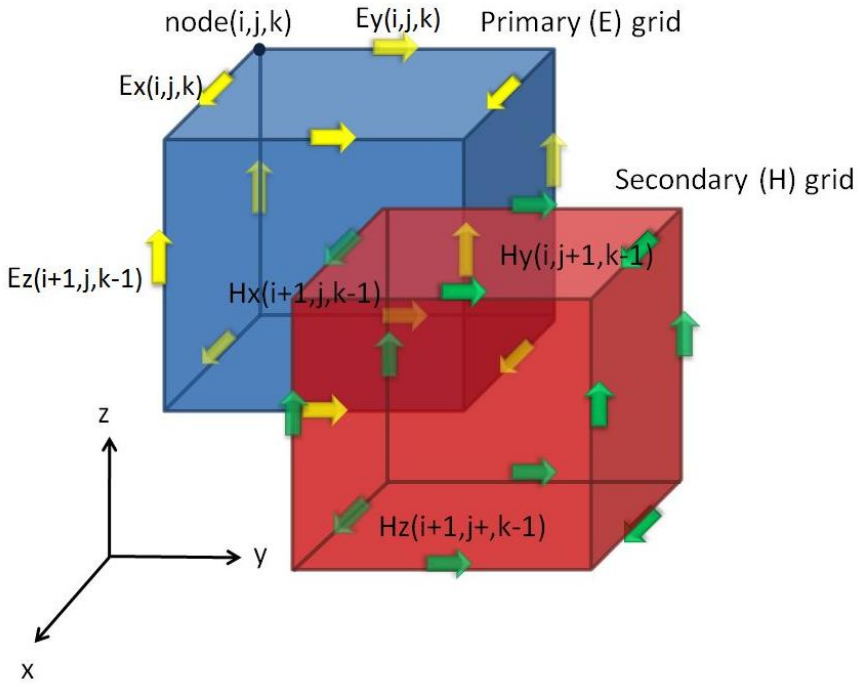

Fig 2.4 3D Basic Element of the FDTD Yee cell [2.54].

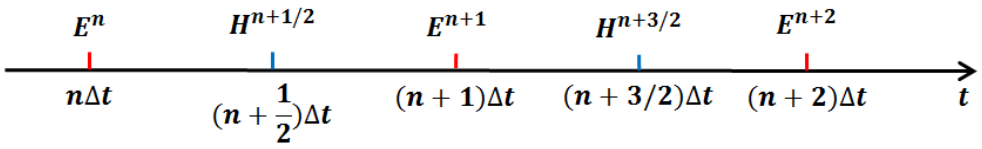

Fig 2.5 Leap-frog scheme in FDTD [2.53].

The time-stepping will stop when a steady state solution or the desired response is obtained[2.53]. At each time step, the equations used to update the E-field components are fully explicit and there is no need to solve a system of linear equations. The technique requires the computer storage and running time proportional to the electrical size of the volume being modelled as well as he mesh grid cell size or the grid resolution.

The mesh grid cell size can be set to any fraction of a wavelength. Increasing or decreasing the mesh resolution, but the time step is inversely proportional to the maximum grid cell size. The mesh grid cell size needs to satisfy the Courant-Friedrichs-Levy (CFL) stability condition (Equation 2.18) [2.55].

$$\Delta t \leq \frac{\sqrt{\varepsilon\mu}}{c\sqrt{\left(\frac{1}{\Delta x}\right)^2 + \left(\frac{1}{\Delta y}\right)^2 + \left(\frac{1}{\Delta z}\right)^2}} \tag{2.18}$$

where c = speed of light in a vacuum, Δx, Δx, and Δz = the cell grid size in the X, Y and Z directions, respectively; ε = permittivity (F/m), μ is the permeability (H/m)

When the cell grid is uniform in all directions, the equation can be reduced to equation 2.19 [2.55].

$$\Delta t \leq \frac{\Delta}{\sqrt{3}c} \tag{2.19}$$

Therefore, a high resolution mesh requires a smaller time step. Since the E-fields need to be evolved in the computational domain evolve over time, if a small time step is employed a larger number of iterations will be required to achieve convergence [2.55]. This is one of the main concerns for this study. In order to calculate the maximum value of energy absorbed in the human tissue the calculation is performed over all the cells. Subsequently the result is averaged over either 1g or 10g of tissue within a given time [2.53]. Different countries and regions follow different standards when considering the SAR. For example in America the FCC emission standard for cell phones is 1.6 W/Kg averaged over 1g of tissue, whereas the IEEE and ICNIRP standards, which apply in Europe, specify 2.0 W/Kg averaged over 10g of tissue. Other researchers have pointed out a SAR of 2 W/Kg averaged over 10g is approximately equivalent to an SAR of 4-6 W/Kg average over 1g [2.20]. Chapter 3 describes an analytical method which was developed to simulate the human phantom exposure to RF fields. The method involves the use of SEMCAD.

2.2.3 Finite Integration Technique

CST Microwave Studio [2.4] is a general-purpose electromagnetic simulator which uses the Finite Integration Technique (FIT) to solve problems in electrostatics and magneto statics. The solver can also be used to handle low frequency and high frequency problems. The FIT was first proposed by Weiland in 1976 [2.56]. The technique yields excellent linear scaling of computational resources with structure size. FIT in the time domain is very similar to the Finite Difference Time domain Technique (FDTD) introduced by Yee in 1966 [2.54]. They are often are called ‘sister’ 3D

computational techniques. FDTD uses approximations to the spatial and the temporal (t) derivatives within Maxwell's equations (i.e. equations 2.14 and 2.15). FIT, on the other hand, FIT employs the integral form of Maxwell's equations [2.55] (i.e. equations 2.20to 2.23).

$$\oint_{\partial A} \vec{E} \cdot d\vec{s} = -\int_{A} \frac{\partial \vec{B}}{dt} \cdot d\vec{A} \tag{2.20}$$

$$\oint_{\partial A} \vec{H} \cdot d\vec{s} = -\int_{A} \left(\frac{\partial \vec{D}}{dt} + \vec{J}\right) \cdot d\vec{A} \tag{2.21}$$

$$\oint_{\partial V} \vec{D} \cdot d\vec{A} = \int_{V} \rho dV \tag{2.22}$$

$$\oint_{\partial V} \vec{B} \cdot d\vec{A} = 0 \tag{2.23}$$

E is the electric field intensity (V/m),

B is the magnetic flux density (W/m ²),

D is the electric flux density (D/m ²),

$\vec{J}$ is the current density(A/m ²),

ρ is the volume charge density (q/ m ³),

A is the element area (m ²),

V is the element volume (m^3).

Like FDTD, FIT is based on creating a suitable mesh system. This involves splitting the computational domain up into many small grid cells, as shown in Fig 2.3

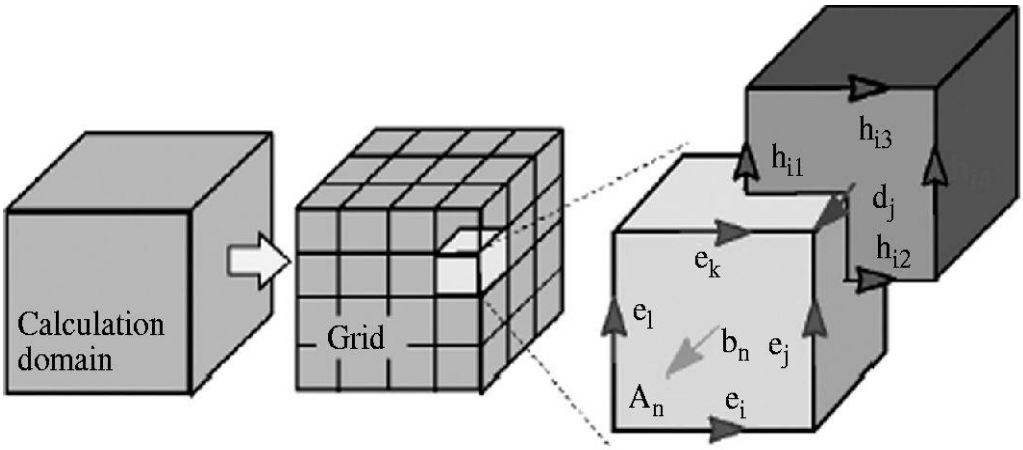

e: electric voltage h: magnetic voltage

b: magnetic flux d: electric flux

Fig 2.6 3D CST microwave studio mesh grids [2.4]

In the case of Cartesian grids, the FIT formulation can be rewritten in the time domain to yield the standard Finite Difference Time Domain (FDTD) method. Upon applying the discretized divergent forms of Faraday's law and Ampere's law we obtain a complete set of Maxwell Grid Equations. Finally the material relations (i.e. dielectric properties) are employed to enable electromagnetic field problems to be solved on the discrete grid space. Classical FDTD methods involve making a staircase approximation to complex geometrical boundaries. However, the FIT can implement the perfect boundary approximation (PBA) along with the thin sheet meshing technique (TST). By making use of these techniques it is possible to produce an accurate model of thin curved and sheets of perfect electrical conductors in additional to staircase approximations [2.55]. The Courant-Friedrichs-Levy (CFL) (equation 2.14) criterion still has to be fulfilled in every single mesh cell to insure that the explicit time integration schemes are conditionally stable [2.55].

2.2.4 Boundary conditions

The perfectly matched layer (PML) boundary conditions used in chapter 3 [2.57] were used. This involves creating a non-physical absorbing medium, adjacent to the external grid boundary, which causes waves of arbitrary frequency and angle of propagation to decay rapidly whilst maintaining the correct wave velocity and impedance within the media from which they originated..

2.2.5 Numerical Simulation Software and Techniques

There are several types of commercially available EMF simulation software, although they are somewhat expensive. Table 2.6 lists some well tested EMF simulation software packages.

Software	Numerical Technique	Company	Information
CONCERTP	FDTD	Vector Fields	http://www.vectorfields.com/
EMPIRE XCcel™	FDTD	IMST GmbH	http://www.empire.de/
FIDELITY™	FDTD	Zeland Software	http://www.zeland.com/
GEMS	FDTD	2COMU	http://www.2comu.com/
SEMCAD X	FDTD	SPEAG	http://www.speag.com/speag/
XFDTD	FDTD	Remcom	http://www.remcom.com/
HFSS™	FEM	Ansoft	http://www.ansoft.com/
CST Microwave Studio	FIT	CST GmbH	http://www.cst.com/
FEKO	MoM/FEM	Electromagnetic Software and Systems	http://www.emss.co.za/
NEC4	MoM	Laurence Livermore National Labs.	https://www.llnl.gov/

Table 2.4 Three-dimensional EMF simulation commercial software packages

The numerical methods used in this thesis have briefed their application and limitations in this section. Considering the EM problem encountered in this research, there are few issues need to address here, when chose a suitable modelling and simulation tools are important for this research. From Table 2.6 it is clear that CST microwave Studio is based on the FEM method, SEMCAD uses the FDTD method, while the NEC4 code is based on MoM. For this reason these software packages are suitable for solving different problems:

- NEC, which uses Moment Method, is most suitable for generating models of wire antennas while the CST Microwave Studio and SEMCAD uses the Finite handle volume problem space with anatomy human phantom implementation.
- Problems involving open boundaries can be accounted for in NEC using MoM, while absorbing boundary conditions have to be introduced in both CST Microwave Studio and SEMCAD.
- The two sets of inhomogeneous human phantoms were devised and compared for the purpose of this thesis. The first phantom was produced in CST Microwave Studio whilst the second was generated in SEMCAD. The MoM is efficient both in terms of cost and computational time, while the packages based on Finite Integration and the Finite Difference Time Domain techniques, namely CST Microwave Studio and SEMCAD, require extra hardware to accelerate the computation of problems involving human bodies in order to avoid excessive processing times.
- CST microwave studio and SEMCAD boundary conditions could not be redefine the dielectric properties, NEC have various realist ground
- A novel MoM-FDTD hybrid approach could provide a possible solution to solve the problems addressed previously.

These summery will hopefully provide a guide to the numerical problem have encountered and solutions was considered and applied.

2.2.6 Equivalence Principles

The Equivalence Principles Method is a three dimensional representation of the surface equivalence theorem for a hybrid numerical method was studied in chapter 5. This theorem replaces electromagnetic sources by equivalent ones; whereby the E-fields

outside an imaginary closed surface are obtained by placing suitable electric and magnetic current densities over an imaginary closed surface that satisfies the desired boundary conditions. These current densities are selected so that the resultant fields are zero within the closed surface. The E-fields should be equal to the radiation produced by the actual electromagnetic sources outside the closed surface.

The technique can be used to obtain the E-fields radiated outside a closed surface by referring to sources enclosed within it. Consider an electromagnetic field (E_1, H_1) in free space, generated by physical electric and magnetic current sources J_1 and M_1. Now assume that J_1 and M_1 are removed, and that a new field (E, H) can be seen to exist inside our imaginary surface. And act as a closed source S, the electric and magnetic currents flowing outside the closed surface S must still satisfy the electromagnetic field boundary conditions on the tangential E and H fields theoretically using Green's theorem as defined by [2.58]:

$$H_s = \hat{n} \times (H_1 - H) \tag{2.24}$$

$$M_s = \hat{n} \times (E_1 - E) \tag{2.25}$$

Where $\hat{n}$ is the unit outward normal vector to the closed source S.

2.3 Conclusion

This thesis is concerned with research into radiofrequency exposure and international human health and safety guidelines. These basic restrictions and reference levels aim to prevent adverse health effects due to EMF exposure. Background theory and relevant research is documented here to enable the reader to develop a basic understanding of what is required for the following chapters of this thesis. Specifically this chapter provides a brief introduction to the commercial simulation software packages and other numerical domestric methods and techniques used in this research. The overall aim of the research presented in this thesis is to use appropriated numerical domestric methods to assess the risk of human exposure to high power HF broadcasting transmitter sites.

References

[2.1] IEEE International Committee, "IEEE C95. 1-1992: IEEE Standard for Safety Levels with Respect to Human Exposure to Radio Frequency Electromagnetic Fields, 3 kHz to 300 GHz, The," *Inc., New York, NY*, vol. 2005, no. April, 1992.

[2.2] International Commission on Non-Ionizing Radiation Protection, "Guidelines for limiting exposure to time-varying electric, magnetic, and electromagnetic fields (up to 300 GHz)," *Heal. Phys.*, vol. 74, no. 4, p. 494, 1998.

[2.3] G. J. Burke, "Numerical Electromagnetics Code NEC-4 Mothod of Moments Part II: Program Description-Theory," 1992.

[2.4] "CST MICROWAVE STUDIO®." CST STUDIO SUITE® http://www.cst.com/.

[2.5] "Virtual Family Phantom®." The IT'IS Foundation http://www.itis.ethz.ch/news-events/news/virtual-population/.

[2.6] SPEAG, "SEMCAD X®." Schmid &Partner Engineering AG http://www.speag.com/.

[2.7] "Basic standard on Short Wave broadcasting (3-30 MHz)," TC106, BSI Technical Cttee GEL/106,, 2007.

[2.8] C. Gandy, "R & D White Paper WHP132," 2006.

[2.9] "Skelton memories," *The British Broadcasting Corporation*. [Online]. Available: http://www.bbceng.info/Operations/transmitter_ops/Reminiscences/skelton/sk1.htm#8.

[2.10] "Vantican Radio." [Online]. Available: http://emfinterface.wordpress.com/2010/07/15/vatican-radio-waves-blamed-for-high-cancer-risk/.

[2.11] T. G. Cooper, S. M. Mann, M. Khalid, and R. P. Blackwell, "Public exposure to radio waves near GSM microcell and picocell base stations.," *J. Radiol. Prot. Off. J. Soc. Radiol. Prot.*, vol. 26, no. 2, pp. 199–211, 2006.

[2.12] German Commission on Radiological Protection, "German Mobile Telecommunication Research Programme (DMF) Deutsches Mobilfunk-Forschungsprogramm Stellungnahme der Strahlenschutzkommission," 2008.

[2.13] International Commission on Non-Ionizing Radiation Protection, "Exposure to high frequency electromagnetic fields, biological effects and health consequences (100 kHz-300 GHz)," *ICNIRP 16/ ...2*, pp. 257–258, 2009.

[2.14] International Commission on Non-Ionizing Radiation Protection, "ICNIRP statement on the 'Guidelines for limiting exposure to time-varying electric,

magnetic, and electromagnetic fields (up to 300 GHz)'.," *Health Phys.*, vol. 97, no. 3, pp. 257–8, 2009.

[2.15] P. Dimbylow, "Assessing the compliance of emissions from MF broadcast transmitters - including exposure guidelines," 2006.

[2.16] P. Dimbylow, "Assessing the compliance of emissions from HF broadcast transmitters - with exposure guidelines," 2006.

[2.17] P. J. Dimbylow, "The calculation of induced currents and absorbed power in a realistic, heterogeneous model of the lower leg for applied electric fields from 60 Hz to 30 MHz.," *Phys. Med. Biol.*, vol. 33, no. 12, pp. 1453–68, Dec. 1988.

[2.18] P. J. Dimbylow, "Current densities in a 2 mm resolution anatomically realistic model of the body induced by low frequency electric fields.," *Phys. Med. Biol.*, vol. 45, no. 4, pp. 1013–22, Apr. 2000.

[2.19] K. Jokela, L. Puranen, and O. P. Gandhi, "Radio frequency currents induced in the human body for medium-frequency/high-frequency broadcast antennas.," *Health Phys.*, vol. 66, no. 3, pp. 237–44, Mar. 1994.

[2.20] International Commission on Non-Ionizing Radiation Protection, "Exposure to high frequency electromagnetic fields, biological effects and health consequences (100 kHz-300 GHz)," *ICNIRP 16/ ...*, 2009.

[2.21] E. D. Mantiply, K. R. Pohl, S. W. Poppell, and J. A. Murphy, "Summary of measured radiofrequency electric and magnetic fields (10 kHz to 30 GHz) in the general and work environment.," *Bioelectromagnetics*, vol. 18, no. 8, pp. 563–577, 1997.

[2.22] E. D. Mantiply, K. R. Pohl, S. W. Poppell, and J. a Murphy, "Summary of measured radiofrequency electric and magnetic fields (10 kHz to 30 GHz) in the general and work environment.," *Bioelectromagnetics*, vol. 18, no. 8, pp. 563–77, Jan. 1997.

[2.23] E. H. ProtectionBranch, "Limits of Human Exposure to Radiofrequency Electromagnetic Fields in the Frequency Range from 3 kHz to 300 GHz Limits of Human Exposure to Radiofrequency Electromagnetic Fields in the Frequency Range from 3 kHz to 300 GHz," 1999.

[2.24] "FCC 02-48: FCC Revision of part 15 of the Commission's rules regarding ultra-wideband transmission systems. ET-Docket 98-153," 2002.

[2.25] R. F. J. Cleveland, *Compliance with FCC exposure guidelines for radiofrequency electromagnetic fields*, vol. 3. IEEE, 2004, pp. 1030–1035.

[2.26] National Council on Radiation Protection and Measurements, "ADVISING THE PUBLIC National Council on Radiation Protection and Measurements A Document for Public Comment," Bethesda, Maryland, 1994.

[2.27] IEEE International Committee on Electromagnetic Safety, "IEEE Standard for Safety Levels with Respect to Human Exposure to Radio Frequency Electromagnetic Fields , 3 kHz to 300 GHz," *Inc., New York, NY*, vol. 2005, no. April, p. 250, 1992.

[2.28] A. ANSI, "IEEE C95. 1-1992: IEEE Standard for Safety Levels with Respect to Human Exposure to Radio Frequency Electromagnetic Fields, 3 kHz to 300 GHz, The," *Inc., New York, NY*, vol. 2005, no. April, 1992.

[2.29] P. J. Dimbylow, "FDTD calculations of the whole-body averaged SAR in an anatomically realistic voxel model of the human body from 1 MHz to 1 GHz.," *Phys. Med. Biol.*, vol. 42, no. 3, pp. 479–90, Mar. 1997.

[2.30] H. Massoudi and C. Durney, "Electromagnetic absorption in multilayered cylindrical models of man," ... *IEEE Trans.*, vol. M, no. 10, 1979.

[2.31] "FDTD electromagnetic and thermal analysis of interstitial hyperthermic applicators," *IEEE Trans. Biomed. Eng.*, vol. 42, no. 10, p. 973, 1995.

[2.32] D. K. Kido, T. W. Morris, J. L. Erickson, D. B. Plewes, and J. H. Simon, "Physiologic changes during high field strength MR imaging.," *AJR. Am. J. Roentgenol.*, vol. 148, no. 6, pp. 1215–8, Jun. 1987.

[2.33] J. R. Jauchem, K. L. Ryan, and M. R. Frei, "Cardiovascular and thermal effects of microwave irradiation at 1 and/or 10 GHz in anesthetized rats.," *Bioelectromagnetics*, vol. 21, no. 3, pp. 159–166, 2000.

[2.34] E. R. Adair and D. R. Black, "Thermoregulatory responses to RF energy absorption.," *Bioelectromagnetics*, vol. Suppl 6, no. September 2002, pp. S17–38, Jan. 2003.

[2.35] International Commission on Non-Ionizing Radiation Protection, "Exposure of humans to electromagnetic fields. Standards and regulations.," *Ann. Ist. Super. Sanita*, vol. 43, no. 3, pp. 260–7, Jan. 2007.

[2.36] T. G. Cooper, S. M. Mann, M. Khalid, and R. P. Blackwell, "Public exposure to radio waves near GSM microcell and picocell base stations.," *J. Radiol. Prot.*, vol. 26, no. 2, pp. 199–211, Jun. 2006.

[2.37] P. J. Dimbylow and S. M. Mann, "SAR calculations in an anatomically realistic model of the head for mobile communication transceivers at 900 MHz and 1.8 GHz.," *Phys. Med. Biol.*, vol. 39, no. 10, pp. 1537–53, Oct. 1994.

[2.38] M. Martínez-Búrdalo, a Martín, a Sanchis, and R. Villar, "FDTD assessment of human exposure to electromagnetic fields from WiFi and bluetooth devices in some operating situations.," *Bioelectromagnetics*, vol. 30, no. 2, pp. 142–51, Feb. 2009.

[2.39] "XFdtd®." Remcom http://www.remcom.com/xf7.

[2.40] I. Chatterjee, M. J. Hagmann, and O. P. Gandhi, "Electromagnetic absorption in a multilayered slab model of tissue under near-field exposure conditions.," *Bioelectromagnetics*, vol. 1, no. 4, pp. 379–388, 1980.

[2.41] I. Chatterjee, "Electromagnetic-energy deposition in an inhomogeneous block model of man for near-field irradiation conditions," *Microw. Theory ...*, pp. 337–340, 1980.

[2.42] M. Hagmann, "Numerical calculation of electromagnetic energy deposition for a realistic model of man," *Microw. Theory ...*, pp. 804–809, 1979.

[2.43] P. Dimbylow and R. Findlay, "The effects of body posture, anatomy, age and pregnancy on the calculation of induced current densities at 50 Hz.," *Radiat. Prot. Dosimetry*, vol. 139, no. 4, pp. 532–8, Jun. 2010.

[2.44] Y. Kawamura and T. Hikage, "Whole-body averaged SAR measurements of postured phantoms exposed to E-/H-polarized plane-wave using cylindrical field scanning," *Antennas ...*, no. 3, pp. 676–679, 2012.

[2.45] "Effects of posture on FDTD calculations of specific absorption rate in a voxel model of the human body," *Phys. Med. Biol.*, vol. 50, no. 16, p. 3825, 2005.

[2.46] "Numerical Electromagnetics Code NEC-4." University of California, Livermore, Ca 94551, Technical Information Dept., Lawrence Livermore National Laboratory.

[2.47] R. Harrington, "Matrix methods for field problems," *Proc. IEEE*, vol. 55, no. 2, p. 136, 1967.

[2.48] G. Marrocco, L. Mattioni, and V. Martorelli, "Naval Structural Antenna Systems for Broadband HF Communications — Part II : Design Methodology for Real Naval Platforms," vol. 54, no. 11, pp. 3330–3337, 2006.

[2.49] R. Harrington, *Field computation by moment methods*. 1993.

[2.50] A. Taflove and M. E. Brodwin, "Numerical Solution of Steady-State Electromagnetic Scattering Problems Using the Time-Dependent Maxwell's Equations," *IEEE Trans. Microw. Theory Tech.*, vol. 23, no. 8, pp. 623–630, Aug. 1975.

[2.51] A. Taflove, "Application of the Finite-Difference Time-Domain Method to Sinusoidal Steady-State Electromagnetic-Penetration Problems," *Ieee Trans. Electromagn. Compat.*, vol. EMC-22, no. 3, pp. 191–202, 1980.

[2.52] G. Mur, "Absorbing boundary conditions for the finite-difference approximation of the time-domain electromagnetic-field equations," *IEEE Trans. Electromag. Compat.*, vol. emc-23, no. 4, p. 377, 1981.

[2.53]R. Guide, "SEMCAD X Reference Guide," *The International Executive*, vol. 30, no. 2. pp. 35–99, 1988.

[2.54] K. . Yee, “Numerical solution of initial boundary value problems involving Maxwell’s equations in isotropic media,” *IEEE Trans. Antennas Propag.*, vol. 14, no. 3, p. 302, 1966.

[2.55] “CST Mircrowave Studio Advance Guide.” .

[2.56] T. Weiland, “A discretization model for the solution of Maxwell’s equations for six-component fields,” *Arch. Elektron. und Uebertragungstechnik*, vol. 31, no. 3, pp. 116–120, 1977.

[2.57] J. Berenger, “A perfectly matched layer for the absorption of electromagnetic waves,” *J. Comput. Phys.*, vol. 114, no. 2, p. 185, 1994.

[2.58] A.Taflove and S. C. Hagness, *Computational Electrodynamics, The Finite-Difference Time-Domain Method*. Boston: Artech House, 2005.